

## Generation and detection of Rydberg wave packets by short laser pulses

G. Alber, H. Ritsch, and P. Zoller

*Institute for Theoretical Physics, University of Innsbruck, A-6020 Innsbruck, Austria*

(Received 28 January 1986)

We discuss the generation and detection of wave packets of Rydberg states by exciting electrons from a low-lying atomic state with a short pulse to a Rydberg series. To observe the motion of the wave packet, we analyze a time-delayed two-photon experiment, where the first laser pulse generates a wave packet, which is then probed by a second short pulse. The two-photon transition probability shows peaks when the time delay between the pulses is a multiple of the classical orbit time. A semiclassical formalism is developed to describe the motion of the wave packet and to analyze the time-delayed two-photon process.

### I. INTRODUCTION

Wave packets, i.e., quantum-mechanical states well localized in space, play a fundamental role in our concepts and understanding of quantum mechanics. They reflect the time evolution of a (localized) coherent superposition of a system, and thus provide the bridge between quantum mechanics and the classical concept of the trajectory (orbit) of a particle.<sup>1</sup>

Observation of wave packets and the study of their motion in quantum-mechanical systems depends on the possibility of generating localized superpositions of eigenstates in a controlled way and the ability to detect the distribution of the wave packet at a later time by a spatially sensitive probe. An experimentally realistic system is electrons in Rydberg states<sup>2</sup> where wave packets corresponding to a coherent superposition of many  $n$  states (with  $n$  the principal quantum number) can be generated by exciting the electrons from a low-lying atomic state with a short laser pulse. Wave packets are formed in this case because (i) the photon absorption from the ground state to the Rydberg states is localized in space in a volume of the size of the ground-state orbital which is small compared with the spatial extent of Rydberg states (whose orbitals for small angular momenta are proportional to  $n^2 a_0$  with  $a_0$  the Bohr radius), and (ii) the laser pulse duration  $\tau$  is short so that its broad bandwidth  $\hbar/\tau$  simultaneously excites many Rydberg states around some mean principal quantum number  $\bar{n}$ :

$$\hbar/\tau \gg \frac{1}{2\pi} \left. \frac{dE_n}{dn} \right|_{n=\bar{n}} = \hbar/T_{E_{\bar{n}}} \quad (1)$$

with  $E_n$  the Rydberg energies and  $T_{E_{\bar{n}}}$  the classical orbit time corresponding to the mean excited energy  $E_{\bar{n}}$ .<sup>1</sup> According to Eq. (1) wave packets are excited when the pulse duration is short compared to the classical orbit time. In this sense Rydberg wave packets can be interpreted as quantum beats between different  $n$  states.<sup>3</sup> Although this concept of generating Rydberg wave packets has been known, at least qualitatively, for many years,<sup>4</sup> a first quantitative discussion has only recently been given by Parker and Stroud.<sup>5</sup> They give an essentially numerical

analysis of the spontaneous emission of an atom excited by a short pulse.

In the present paper we give a discussion of the controlled generation, motion, and detection of Rydberg wave packets with short laser pulses using a semiclassical formalism.<sup>1,6-8</sup> In particular, we give a detailed analysis of a two-photon process with two time-delayed laser pulses where the first pulse generates the Rydberg wave packet whose motion is probed by a second short pulse. This detection scheme provides us with a time- and space-sensitive probe since the absorption of a probe laser photon can only occur near the inner turning point of the classical Kepler orbit, where the acceleration of the electron is largest. The probability of the two-photon transition as a function of the time delay  $\Delta t$  between both laser pulses will show peaks whenever  $\Delta t$  is a multiple of the classical orbit time  $T_{E_{\bar{n}}}$ . Finally, we believe that our analysis is also interesting from the point of view of multiphoton absorption in short laser pulses.

The paper is organized as follows. In Sec. II we discuss the generation of Rydberg wave packets by short laser pulses using perturbation theory and give a simple semiclassical analysis of the motion of the wave packet. Section III discusses the detection of the motion of Rydberg wave packets in a time-delayed two-photon process.

### II. LASER EXCITATION OF RYDBERG WAVE PACKETS

We consider an atom with a single valence electron. This electron is excited from an initial state  $|i\rangle$  with energy  $E_i$  to a series of Rydberg states by a short laser pulse of duration  $\tau_a$  and mean frequency  $\omega_a$ . The center of the pulse reaches the atom at time  $t_a$ . The electric field at the position of the atom  $\mathbf{x}=\mathbf{0}$  can be written in the form

$$\mathbf{E}(\mathbf{x}=\mathbf{0}, t) = \mathcal{E}_a(t) \boldsymbol{\epsilon}_a e^{-i\omega_a t} + \text{c.c.} \quad (2)$$

with  $\boldsymbol{\epsilon}_a$  a polarization vector and  $\mathcal{E}_a(t)$  a slowly varying complex amplitude which we assume to be a Gaussian,

$$\mathcal{E}_a(t) = \mathcal{E}_a^{(0)} \exp[-4(\ln 2)(1+i\varphi_a)(t-t_a)^2/\tau_a^2]. \quad (3)$$

$\varphi_a$  describes a phase change during the pulse.  $\tau_a$  is the

full width at half maximum of the pulse duration of the electric field. The Fourier transform of  $\mathcal{E}_a(t)$  is defined as

$$\begin{aligned}\tilde{\mathcal{E}}(\Delta\omega) &= \int_{-\infty}^{+\infty} dt \mathcal{E}_a(t) e^{i\Delta\omega(t-t_a)} \\ &= \mathcal{E}_a^{(0)} \left[ \frac{\pi\tau_a^2}{4(\ln 2)(1+i\varphi_a)} \right]^{1/2} \\ &\quad \times \exp \left[ -\frac{(1-i\varphi_a)(\Delta\omega)^2\tau_a^2}{16(\ln 2)(1+\varphi_a^2)} \right].\end{aligned}\quad (4)$$

For weak fields, neglecting saturation effects, we find in lowest-order perturbation theory and in the rotating-wave approximation (RWA) for the electron wave function

$$|\psi(t)\rangle = |i\rangle e^{-iE_i t/\hbar} + |\psi_i^{(a)}(t)\rangle \quad (5)$$

with

$$\begin{aligned}|\psi_i^{(a)}(t)\rangle &= \frac{i}{\hbar} \int_{-\infty}^t dt' e^{-iH_A(t-t')/\hbar} \boldsymbol{\mu} \cdot \boldsymbol{\epsilon}_a \mathcal{E}_a(t') |i\rangle \\ &\quad \times e^{-i(E_i + \hbar\omega_a)t'/\hbar} \\ &= \sum_{\substack{n=n_0 \\ l, m_l}} |nlm_l\rangle e^{-iE_n t/\hbar} a_{nlm_l \leftarrow i}^{(a)}(t).\end{aligned}\quad (6)$$

Here  $H_A$  is the atomic Hamiltonian;  $|nlm_l\rangle$  are Rydberg states with energy  $E_n$ ;  $l$  and  $m_l$  are angular quantum numbers and  $a_{nlm_l \leftarrow i}^{(a)}(t)$  are Rydberg amplitudes. We ignore the fine structure of the atom. For times  $t \geq t_a + \tau_a$  after the laser pulse has passed the atom these amplitudes are given by

$$a_{nlm_l \leftarrow i}^{(a)}(\infty) = \frac{i}{\hbar} \langle nlm_l | \boldsymbol{\mu} \cdot \boldsymbol{\epsilon}_a | i \rangle \tilde{\mathcal{E}}_a(\delta_{in}^{(a)}) e^{i\delta_{in}^{(a)} t_a} \quad (7)$$

where  $\tilde{\mathcal{E}}_a(\delta_{in}^{(a)})$  the spectral density (4) evaluated at the detuning  $\delta_{in}^{(a)} = (E_n - E_i - \hbar\omega_a)/\hbar$ . If the laser pulse is short, the second term in Eq. (5) describes a wave packet corresponding to a coherent superposition of Rydberg states. Note, however, that this is a wave packet only as far as the radial motion is concerned. Since only few angular momenta  $l$  contribute to the sum in Eq. (6) according to dipole selection rules, there is no localization in the angular variables  $\theta$  and  $\phi$ . To discuss the structure of the radial wave packet we rewrite the sum over  $n$  states in Eq. (6) with the help of the Poisson-sum formula<sup>6-8</sup>

$$\sum_{n=n_0}^{\infty} f(n) = \sum_{m=-\infty}^{+\infty} \int_{n_0}^{\infty} dn f(n) e^{i2\pi mn}. \quad (8)$$

For  $t > t_a + \tau_a$  we thereby obtain

$$\begin{aligned}\langle \mathbf{x} | \psi_i^{(a)}(t) \rangle &= \sum_{l, m_l} \frac{i}{\hbar} \left[ \int_{E_{n_0}}^{\infty} dE R_{El}(r) Y_l^{m_l}(\theta, \phi) e^{-iE(t-t_a)/\hbar} \boldsymbol{\mu}_{Elm_l, i} \cdot \boldsymbol{\epsilon}_a \tilde{\mathcal{E}}_a(\delta_{iE}^{(a)}) \right. \\ &\quad \left. + \sum_{\substack{m=-\infty \\ (m \neq 0)}}^{+\infty} e^{i2\pi m \alpha_l} \int_{E_{n_0}}^0 dE R_{El}(r) Y_l^{m_l}(\theta, \phi) e^{-iE(t-t_a)/\hbar} \boldsymbol{\mu}_{Elm_l, i} \cdot \boldsymbol{\epsilon}_a \tilde{\mathcal{E}}_a(\delta_{iE}^{(a)}) e^{2\pi i m \nu} \right] e^{-i(E_i + \hbar\omega_a)t_a/\hbar},\end{aligned}\quad (9)$$

where  $E = -\mathcal{R}/\nu_l^2$ ,  $\nu_l = n - \alpha_l$  with  $\alpha_l$  the quantum defect, which depends on  $l$  but is approximately independent of  $n$ .  $R_{El}(r)$  are radial wave functions normalized on the energy scale. For  $E < 0$  these energy-normalized wave functions are related to the usual unit-normalized bound-state functions  $R_{nl}(r)$  by

$$R_{El}(r) = \left[ \frac{dE}{dn} \right]^{-1/2} R_{nl}(r) \quad \text{with} \quad \frac{dE}{dn} = \frac{2\mathcal{R}}{\nu_l^3}. \quad (10)$$

In Eq. (9)  $\boldsymbol{\mu}_{Elm_l, i}$  denotes the matrix element from the initial state  $|i\rangle$  to the energy-normalized excited state with energy  $E$ . It is known that these matrix elements are slowly varying functions of the energy  $E$  across the Rydberg threshold<sup>9,10</sup> and thus—consistent with the RWA—can be approximated by constants in the integrals of Eq. (9).

Furthermore, the spectral density of the exciting pulse is concentrated in an energy band  $E_i + \hbar\omega_a - \hbar/\tau_a \leq E \leq E_i + \hbar\omega_a + \hbar/\tau_a$  with the maximum centered at a mean energy  $E_{\bar{n}} = E_i + \hbar\omega_a$ . If we are interested in the ra-

dial motion for values of  $r$  between (and not too close to) the classical turning points  $r_1 \leq r \leq r_2$  we can approximate the radial wave function  $R_{El}(r)$  by its WKB form<sup>1</sup>

$$R_{El}(r) = \frac{1}{r} \frac{1}{(\mathcal{R}a_0)^{1/2}} \frac{1}{\sqrt{\pi}} \frac{\cos \left[ \frac{1}{\hbar} \int_{r_1}^r dr' p(r') - \pi/4 \right]}{[p(r)a_0/\hbar]^{1/2}}. \quad (11a)$$

The radial electron momentum is thereby given by

$$p(r) = \left[ 2\mu[E - V(r)] - \frac{\hbar^2(l+1/2)^2}{r^2} \right]^{1/2} \quad (11b)$$

with  $p(r_1) = p(r_2) = 0$ .  $V(r)$  is a model potential for the alkali-metal atom, which asymptotically goes like a Coulomb potential and  $\mu$  is the reduced electron mass.

By evaluating the integrals of Eq. (9) in the stationary-phase approximation we find that the center of the wave packet  $r(t)$  follows the classical trajectory of a particle moving in the potential  $V(r)$ . Such a stationary-phase

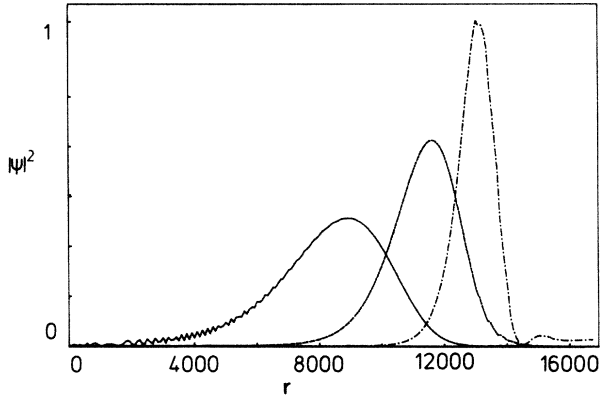


FIG. 1. Radial Rydberg wave packet as a function of  $r$  (in units of the Bohr radius  $a_0$ ) at times  $\Delta t = t - t_a = \frac{1}{9}T_{E_{\bar{n}}}, \frac{2}{9}T_{E_{\bar{n}}}, \frac{3}{9}T_{E_{\bar{n}}}$ . The laser pulse of duration 8 psec ( $\varphi_a = 0$ ) excites a hydrogen  $s$  state to the Rydberg  $p$  series around  $\bar{n} = 85T_{E_{\bar{n}}} = 94$  psec. The wave packet is calculated using a WKB solution for the Coulomb functions (Ref. 1).

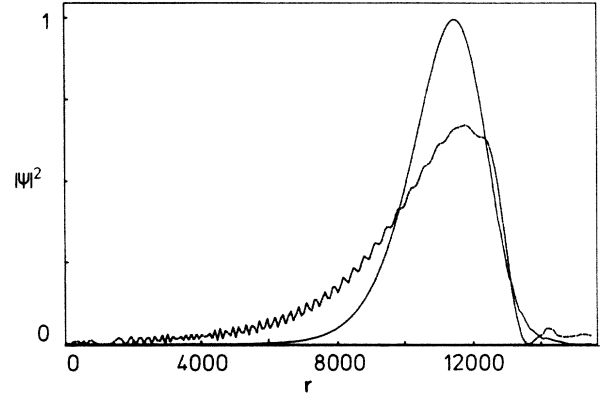


FIG. 2. Radial Rydberg wave packet for  $\Delta t = \frac{2}{9}T_{E_{\bar{n}}}$  and  $(1 + \frac{2}{9})T_{E_{\bar{n}}}$ . For the other parameters see Fig. 1.

evaluation is expected to represent  $\langle \mathbf{x} | \psi_i^{(a)}(t) \rangle$  adequately as long as condition (1) is fulfilled and  $t - t_a \gg \tau_a$ . In particular, if the spectral density of the exciting laser pulse is concentrated in the continuum (i.e.,  $E_i + \hbar\omega_a - \hbar/\tau_a > 0$ ) the dominant contribution to Eq. (9) comes from the points of stationary phase in the  $m = 0$  integral, where

$$\int_{r_1}^{r(t)} \frac{\mu}{p(r')} dr' = t - t_a \quad (E > 0). \quad (12a)$$

Equation (12a) is the classical equation of motion of a particle of energy  $E > 0$ , which escapes to infinity. If the laser pulse excites bound Rydberg states ( $E_i + \hbar\omega_a - \hbar/\tau_a < 0$ ), then the terms with  $m \neq 0$  describe the periodic motion of a bound electron. The stationary phase condition now becomes

$$\pm \int_{r_1}^{r(t)} \frac{\mu}{p(r')} dr' = t - (t_a + mT_E), \quad m = 0, 1, 2, \dots \quad (12b)$$

The orbiting time, which corresponds to a bound orbit of energy  $E$ , is thereby given by<sup>1</sup>

$$T_E = \pi \frac{\hbar}{\mathcal{R}} (-E/\mathcal{R})^{-3/2}. \quad (13)$$

The index  $m$  in Eq. (12b) characterizes the  $m$ th return of the wave packet to a particular point  $r$ .

The number of Rydberg states contributing to the wave packet can be estimated from

$$\Delta n \simeq \frac{dn}{dE} \Big|_{E=E_{\bar{n}}} \left[ 2\pi \frac{\hbar}{\tau_1} \right] = T_{E_{\bar{n}}}/\tau_1 \gg 1, \quad (14)$$

and is seen to be of the order of the ratio between the classical orbit time and the pulse length of the laser. Figures 1 and 2 show the motion of the radial wave packet when a Gaussian laser pulse with  $\tau_a = 8$  psec ( $\varphi_a = 0$ ) excites a Rydberg wave packet with  $\bar{n} = 85$  and a classical orbit time  $T_{E_{\bar{n}}} = 94$  psec. In Fig. 1 we plot the wave packet for times  $t - t_a \equiv \Delta t = \frac{1}{9}T_{E_{\bar{n}}}, \frac{2}{9}T_{E_{\bar{n}}}, \frac{3}{9}T_{E_{\bar{n}}}$ . Note that the contraction of the wave packet is due to the slowing down of the electron motion near the outer classical turning point. Figure 2 compares the wave packet at time  $\Delta t = \frac{2}{9}T_E$  and  $(1 + \frac{2}{9})T_E$  (i.e., one classical orbit time later). As is apparent from Fig 2, the wave packet spreads with increasing time. Using a phase change during the pulse ( $\varphi_a \neq 0$ ) it is possible to influence the relative phases of the Rydberg amplitudes (7) and to create a wave packet, which contracts during the first few classical orbit times until it decays (see also Sec. III).

### III. DETECTION OF THE WAVE PACKET BY TIME-DELAYED TWO-PHOTON PROCESSES

To detect the motion of the wave packet we suggest a time-delayed two-photon absorption-emission technique: a first pulse  $\mathcal{E}_a(t)$  excites the Rydberg wave packet at time  $t_a$ , which is probed at a later time  $t_b > t_a + \tau_a$  by a second short pulse  $\mathcal{E}_b(t)$  of duration  $\tau_b$  and mean frequency  $\omega_b$ . The simplest version of such a two-photon detection scheme is a Raman process where the second pulse deexcites the Rydberg electron by induced emission to a (low-lying) bound state  $|f\rangle$  with energy  $E_f$ . Using perturbation theory, the probability of finding the electron in state  $|f\rangle$  at the time  $t > t_b + \tau_b$ , after the probe pulse has passed the atom, is

$$P_{f \leftarrow i}(t) = \left| \frac{i}{\hbar} \int_{-\infty}^t dt' e^{i(E_f + \hbar\omega_b)t'/\hbar} \langle f | \boldsymbol{\mu} \cdot \boldsymbol{\epsilon}_b^* | \psi_i^{(a)}(t') \rangle \mathcal{E}_b^*(t') \right|^2. \quad (15)$$

We can rewrite Eq. (15) in the form

$$P_{f \leftarrow i}(t) = \int d^3x_1 \int d^3x_2 \int_{-\infty}^t dt_1 \int_{-\infty}^t dt_2 S(\mathbf{x}_1, t_1; \mathbf{x}_2, t_2) \psi_i^{(a)}(\mathbf{x}_1, t_1) [\psi_i^{(a)}(\mathbf{x}_2, t_2)]^* \quad (16a)$$

with the sensitivity function of our detection process

$$S(\mathbf{x}_1, t_1; \mathbf{x}_2, t_2) = \langle \mathbf{x}_1 | \boldsymbol{\mu} \cdot \boldsymbol{\epsilon}_b | f \rangle \langle f | \boldsymbol{\mu} \cdot \boldsymbol{\epsilon}_b^* | \mathbf{x}_2 \rangle e^{i(E_f + \hbar\omega_b)(t_1 - t_2)/\hbar} \mathcal{E}_b^*(t_1) \mathcal{E}_b(t_2). \quad (16b)$$

As is apparent from Eq. (16b),  $S(\mathbf{x}_1, t_1; \mathbf{x}_2, t_2)$  is only significant in the regions  $|\mathbf{x}_1|, |\mathbf{x}_2| \leq a_0$  and  $|t_1 - t_2|, |t_2 - t_b| < \tau_b$  and is therefore well localized in time and space as long as all distances (times) of interest are much larger than the Bohr radius (pulse duration).

In other words, the spatial localization of the induced-photon-emission process near the inner turning point of the classical orbit provides a space- and time-sensitive probe of the wave packet. As we already noted in Sec. II this is reflected in the approximate energy independence of the dipole matrix elements  $\boldsymbol{\mu}_{E,f}$  ( $\boldsymbol{\mu}_{E,i}$ ) between  $|f\rangle$  ( $|i\rangle$ ) and the energy-normalized Rydberg-state wave functions  $|E\rangle$ .<sup>9,10</sup> This picture of the time-delayed two-photon Raman process as a spatial- and time-sensitive probe of the Rydberg wave packet can be brought out more clearly if we write Eq. (15) in the form (for simplicity we suppress in the following the angular momentum quantum numbers)

$$P_{f \leftarrow i}(t) = \left| \sum_n [a_{n \leftarrow f}^{(b)}(\infty)]^* a_{n \leftarrow i}^{(a)}(\infty) \right|^2 = |\langle \psi_f^{(b)}(t) | \psi_i^{(a)}(t) \rangle|^2. \quad (17)$$

Here  $|\psi_f^{(b)}(t)\rangle$  is a wave packet [compare Eq. (6)] which is created if we excite Rydberg states from state  $|f\rangle$  with a laser pulse  $\mathcal{E}_b(t)$ . In Eq. (17) we assume that  $t > t_b + \tau_b$  and  $t_b - \tau_b > t_a + \tau_a$ . As the wave function  $|\psi_f^{(b)}(t)\rangle$  is localized near the nucleus, the overlap  $|\langle \psi_f^{(b)}(t) | \psi_i^{(a)}(t) \rangle|$  will be large when the time delay  $t_b - t_a$  between the pulses is a multiple of the classical orbit time  $T_{E_n}$ . The population of state  $|f\rangle$ ,  $P_{f \leftarrow i}$  as a function of  $t_b - t_a$  will thus display peaks at  $t_b - t_a \simeq m T_{E_n}$  where  $m = 1, 2, \dots$  corresponds to the first, second, etc. return of the wave packet  $|\psi_i^{(a)}(t)\rangle$  to the inner turning point; at least for times where the wave packet  $|\psi_i^{(a)}(t)\rangle$  has a spread which is small compared with the dimension of the classical orbit. Note that for  $\tau_b \gg T_{E_n}$  Eq. (17) is proportional to the populations of the Rydberg states.

According to Eq. (17), the transition probability  $P_{f \leftarrow i}$  is proportional to the square of the modulus of

$$I(t_b, t_a) = \sum_{n=n_0}^{\infty} \frac{2\mathcal{R}}{\mathcal{V}(n)} \tilde{\mathcal{E}}_b^*(\delta_{fn}^{(b)}) \tilde{\mathcal{E}}_a(\delta_{in}^{(a)}) e^{-i\delta_{fn}^{(b)} t_b + i\delta_{in}^{(a)} t_a} + \int_0^{\infty} dE \tilde{\mathcal{E}}_b^*(\delta_{fE}^{(b)}) \tilde{\mathcal{E}}_a(\delta_{iE}^{(a)}) e^{-i\delta_{fE}^{(b)} t_b + i\delta_{iE}^{(a)} t_a}. \quad (18)$$

Using the Poisson-sum formula (8) we find

$$I(t_b, t_a) = \sum_{\substack{m \neq 0, \\ m = -\infty}}^{\infty} e^{i2\pi m \alpha} \int_{E_0}^0 dE \tilde{\mathcal{E}}_b^*(\delta_{fE}^{(b)}) \tilde{\mathcal{E}}_a(\delta_{iE}^{(a)}) \times e^{-i\delta_{fE}^{(b)} t_b + i\delta_{iE}^{(a)} t_a} \times \exp(2\pi i m / \sqrt{-E/\mathcal{R}}), \quad (19)$$

where in agreement with our discussion of Eqs. (12) we will identify the  $m = 1, 2, \dots$  term with the contribution due to the first, second return of the wave packet  $|\psi_i^{(a)}(t)\rangle$  to its inner turning point. We have left out the term with  $m = 0$  in Eq. (19) (including the continuum contribution) assuming  $t_a - t_b \geq T_{E_n} \gg \tau_a, \tau_b$  [see the discussion following Eq. (9)]. Evaluating the integral in Eq. (19) by a stationary-phase approximation we obtain

$$I(t_b, t_a) = \sum_{m=1}^{\infty} e^{i(\pi/4)} \left[ \frac{2\pi}{\left| \frac{d^2\phi}{dE^2} \right|_{E=E_s^{(m)}}} \right]^{1/2} \times \tilde{\mathcal{E}}_b^*(\delta_{fE_s^{(m)}}^{(b)}) \tilde{\mathcal{E}}_a(\delta_{iE_s^{(m)}}^{(a)}) e^{i\phi(E_s^{(m)})} \quad (20a)$$

with the phase

$$\phi(E) = -(E_i + \hbar\omega_a - E)t_a / \hbar + (E_f + \hbar\omega_b - E)t_b / \hbar + 2\pi m [\alpha + (-E/\mathcal{R})^{-1/2}], \quad (20b)$$

and the points of stationary phase  $E_s^{(m)}$  determined by

$$\hbar \frac{d\phi}{dE} \Big|_{E=E_s^{(m)}} \equiv -(t_b - t_a) + m T_{E_s^{(m)}} = 0 \quad (m = 1, 2, \dots). \quad (20c)$$

The second derivative of the phase is given by

$$\frac{d^2\phi}{dE^2} \Big|_{E=E_s^{(m)}} = \frac{3}{2} \pi m (-E_s^{(m)}/\mathcal{R})^{-5/2} \mathcal{R}^{-2} > 0. \quad (20d)$$

Equation (20a) is expected to be a good approximation to Eq. (18) as long as  $t_b - t_a \gg \tau_a, \tau_b$  and condition (1) is fulfilled.

For a given time delay  $\Delta t = t_b - t_a$  [Eq. (20c)] determines the stationary energies  $E_s^{(m)} = -\mathcal{R}(m\pi\hbar/\mathcal{R}\Delta t)^{2/3}$  with  $m = 1, 2, \dots$ . The dominant contribution to the sum in Eq. (20a) comes from stationary energies with  $E_s^{(m)} \simeq E_i + \hbar\omega_a \simeq E_f + \hbar\omega_b = E_n$ , which implies that  $\Delta t = m T_{E_n}$ , i.e., the time delay between the exciting and probing laser is a multiple of the mean classical orbit

time. The number of  $m$  values  $\Delta m$  which contribute to the sum in Eq. (20a) for a given  $\Delta t$  is determined by the condition  $|E_s^{(m+\Delta m)} - E_s^{(m)}| = \hbar/\tau_a$ . This way we obtain approximately  $\Delta m \approx \frac{1}{2} [1/(|E_{\bar{n}}| \tau_a/\hbar)] \Delta t/T_{E_{\bar{n}}}$ . For small time delays, i.e.,  $\Delta t/T_{E_{\bar{n}}} < \frac{2}{3} (|E_{\bar{n}}| \tau_a/\hbar)$ , we therefore expect well-isolated peaks for the transition probability  $P_{f \leftarrow i}$  at the positions  $\Delta t/T_{E_{\bar{n}}} = 1, 2, \dots$ . The shape of these peaks is thereby determined by the Fourier transform of the pulse envelopes. For large time delays, i.e.,  $\Delta t/T_{E_{\bar{n}}} \gg \frac{2}{3} (|E_{\bar{n}}| \tau_a/\hbar)$ , many  $m$  values contribute to Eq. (20a), giving rise to a complicated dependence of  $P_{f \leftarrow i}$  on  $\Delta t$ .

In Fig. 3 we plot  $P_{f \leftarrow i}$  as a function of  $\Delta t = t_b - t_a$  for a pulse duration  $\tau_a = \tau_b = 5$  psec. The time delay  $\Delta t$  is measured in units of the classical orbit time  $T_{E_{\bar{n}}} = 94$  psec ( $\bar{n} = 85$ ). The solid curve was obtained by summing over the  $n$  states using Eq. (18). The dashed line corresponds to the semiclassical approximation Eq. (20). The first few recurrences of the wave packet lead to isolated peaks at time delays  $\Delta t/T_{E_{\bar{n}}} = 1, 2$ . In Eq. (20a) these peaks correspond to contributions from  $m = 1, 2$ . With increasing time delay the peaks broaden until they finally overlap giving rise to a complicated interference pattern in the time evolution. Equation (20a) is seen to be an excellent approximation to the sum (18). For larger times Eq. (20a) smoothly interpolates the rapid oscillations of Eq. (18). This is due to the fact that the stationary phase approximation of Eq. (20a), which is valid for  $t_b - t_a \gg \tau_a, \tau_b$ , automatically averages out the rapid oscillations on the time scales  $\tau_a, \tau_b$ , which are still contained in Eq. (18).

Figure 4 shows  $P_{f \leftarrow i}$  as a function of  $\Delta t$  for a laser-pulse duration of  $\tau_a = \tau_b = 10$  psec, the other parameters being the same as in Fig. 3. The long laser pulse leads to relatively narrow peaks which broaden very slowly when compared with Fig. 3. Equation (20a) is seen to be a poor

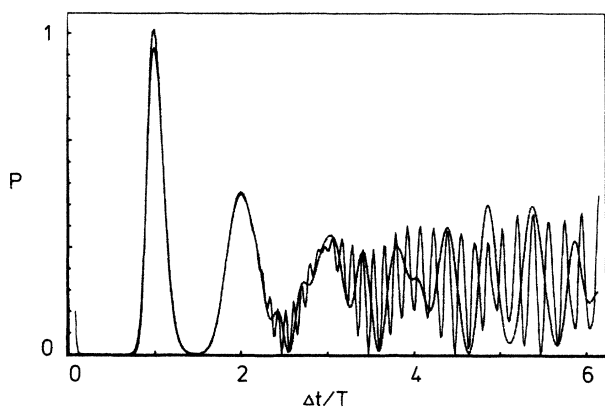


FIG. 3. Two-photon Raman transition probability  $P_{f \leftarrow i}$  (in arbitrary units) for an  $s \rightarrow p \rightarrow s$  transition as a function of the time delay  $\Delta t$  between the two laser pulses measured in units of the classical orbit time  $T_{E_{\bar{n}}} = 94$  psec corresponding to  $\bar{n} = 85$ . The laser pulse duration is  $\tau_a = \tau_b = 5$  psec ( $\varphi_a = \varphi_b = 0$ ). Both lasers are tuned to exact resonance  $E_i + \hbar\omega_a = E_f + \hbar\omega_b$ . The dashed line corresponds to Eq. (20), the solid line is a calculation based on Eq. (18) summing from  $n = 60$  to 120.

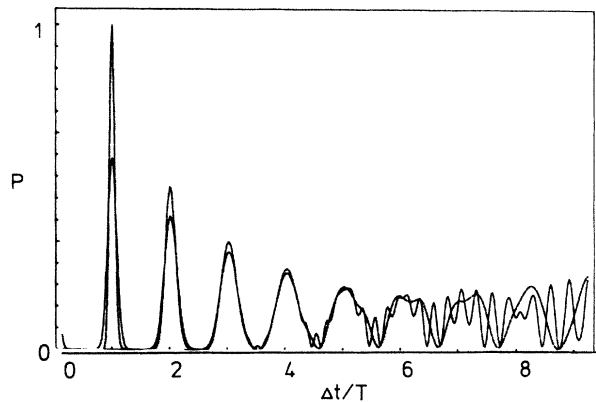


FIG. 4. Same as Fig. 3 with  $\tau_a = \tau_b = 10$  psec.

approximation for short times which is not unexpected since  $T_{E_{\bar{n}}}/\tau_a \approx 9.5$  is not a large parameter.

The possibility of influencing the widths and heights of the peaks in the signal  $P_{f \leftarrow i}$  as a function of  $\Delta t$  by a change of the laser phase during the pulse ( $\tau_a = \tau_b = 12.5$  psec,  $\varphi_a = -\varphi_b = 1$ ) is shown in Fig. 5. Note that the sharpest peak occurs for  $\Delta t = 2T_{E_{\bar{n}}}$  ( $\bar{n} = 85$ ). Finally in Fig. 6 we plot the time dependence of the transition probability for a time delay  $\Delta t$  up to 35 classical orbit times ( $\bar{n} = 85$ ) and  $\tau_a = \tau_b = 8$  psec. As has been first discussed by Parker and Stroud,<sup>4</sup> a revival of the wave packets can be observed.

It is interesting to note that not only the matrix elements  $\mu_{E,i}$  ( $\mu_{E,f}$ ) from Rydberg states to low-lying bound states are approximately constant as a function of  $E$  but also matrix elements describing the ionization from the Rydberg state to the continuum.<sup>9,10</sup> This arises from the fact that even for a bound-free transition the absorption of a photon is localized in space near the inner turning point of the classical orbit, as is well known from a semiclassical theory of radial matrix elements.<sup>11,12</sup> Thus the ionization probability in a two-photon ionization experiment with time-delayed pulses will show a structure simi-

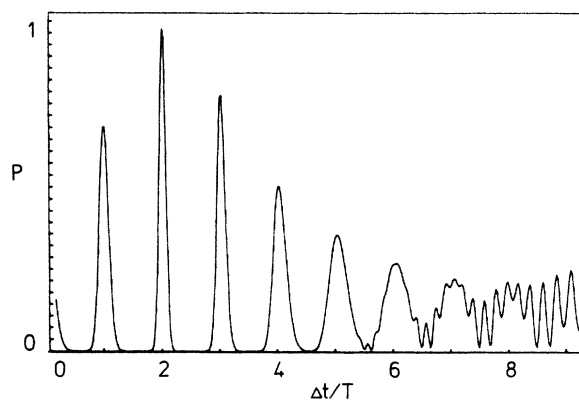


FIG. 5. Same as Fig. 3 but the lasers are phase modulated with  $\varphi_a = -\varphi_b = 1$ . The pulse durations are  $\tau_a = \tau_b = 12.5$  psec.

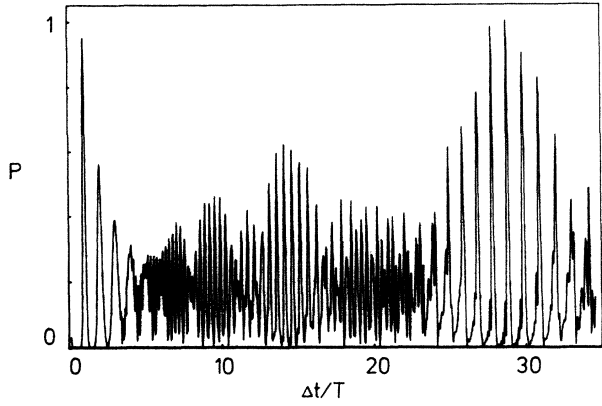


FIG. 6. Same as Fig. 3 with  $\tau_a = \tau_b = 8$  psec. A revival of the wave packet is observed (Ref. 4).

lar to the one we have discussed for the Raman experiment.

Our discussion so far has emphasized the quasiclassical features of the motion of wave packets. Purely quantum-mechanical effects are, for example, interference of wave-packet wave functions. In our context this can be observed by (coherently) exciting two Rydberg wave packets from state  $|i\rangle$ : a first one  $|\psi_i^a(t)\rangle$  at time  $t_a$  with a laser pulse  $\mathcal{E}_a(t)$  and a second one  $|\psi_i^{a'}(t)\rangle$  at time  $t_{a'}$  with an electric field amplitude  $\mathcal{E}_{a'}(t)$  (for simplicity we assume  $\tau_a = \tau_{a'}$  and  $\omega_a = \omega_{a'}$ ). Suppose now that the second wave packet is created at a time  $t_{a'} \simeq t_a + T_{E_{\bar{n}}}$ , when the first wave packet returns for the first time to its inner turning point. Depending on the relative phases between  $|\psi_i^a(t)\rangle$  and  $|\psi_i^{a'}(t)\rangle$ , there will be constructive or destructive interference between the electron wave packets. This can be detected by a third probe pulse  $\mathcal{E}_b(t)$  at time  $t_b > t_a + \tau_a$ , which induces a transition to a final state  $|f\rangle$ . Assuming depletion of  $|i\rangle$  to be negligible we obtain in perturbation theory [compare Eq. (17)]

$$P_{f \leftarrow i}(t) = \left| \sum_{\bar{n}} [a_{n \leftarrow f}^{(b)}(\infty)]^* [a_{n \leftarrow i}^{(a)}(\infty) + a_{n \leftarrow i}^{(a')}(\infty)] \right|^2 \\ = |\langle \psi_f^b(t) | [ |\psi_i^a(t)\rangle + |\psi_i^{a'}(t)\rangle ] |^2 \quad (21)$$

with  $t > t_b + \tau_b$ . By varying the relative phase between  $\mathcal{E}_a(t)$  and  $\mathcal{E}_{a'}(t)$  it is possible to change the relative phases between  $|\psi_i^a(t)\rangle$  and  $|\psi_i^{a'}(t)\rangle$ . Figure 7 shows  $P_{f \leftarrow i}$  as a function of the time delay  $t_b - t_a$  ( $t_{a'} = t_a + T_{E_{\bar{n}}}$  with  $\bar{n} = 85$ ) for two values of the relative phase between  $\mathcal{E}_a(t)$  and  $\mathcal{E}_{a'}(t)$  to obtain (optimum) constructive and destructive interference. In the case of constructive interference (solid line)  $P_{f \leftarrow i}$  consists of well-pronounced peaks repeating themselves with the classical orbit time. For destructive interference (dashed line) there is almost complete cancellation between  $|\psi_i^a(t)\rangle$  and  $|\psi_i^{a'}(t)\rangle$  so that the transition probability  $P_{f \leftarrow i}$  is small for all time delays.

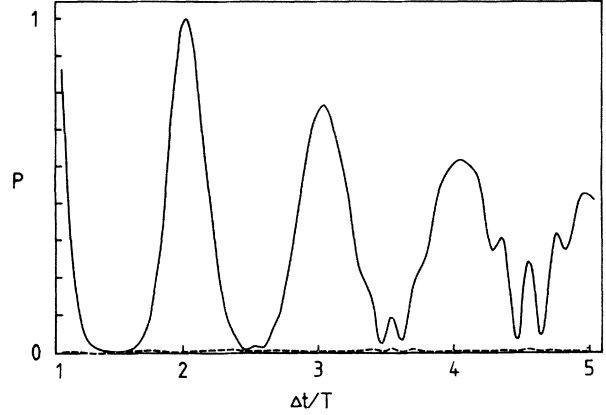


FIG. 7. Interference between two wave packets  $|\psi_i^a(t)\rangle$  and  $|\psi_i^{a'}(t)\rangle$ , created at times  $t_a$  and  $t_{a'} = t_a + T_{E_{\bar{n}}}$  ( $\bar{n} = 85$ ), respectively, is probed as a function of the time delay by a third pulse inducing a Raman transition. The transition probability is plotted as a function of the time delay  $\Delta t = t_b - t_a$  where the global phase between the two exciting pulses [compare Eq. (21)] has been chosen to obtain optimum constructive (solid line) and destructive (dashed line) interference.  $\tau_a = \tau_{a'} = \tau_b = 12.5$  psec;  $\varphi_a = \varphi_{a'} = \varphi_b = 0$ .

#### IV. CONCLUSIONS

We have investigated the excitation of Rydberg states by short laser pulses, which offers the possibility to generate an electronic wave packet in an atom. This is due to the fact that the photon absorption from a low-lying atomic state to a Rydberg state by a short laser pulse is well localized in space and time in comparison with the spatial extension and the classical orbit time of the (mean) excited Rydberg orbit. However, the motion of the electron is well localized only with respect to its radial coordinate. Due to dipole selection rules only a few angular momenta are usually excited by a laser pulse so that the electron motion with respect to the angular variables  $\theta$  and  $\phi$  is delocalized.

In particular we studied a convenient method for probing the excited radial wave packet by a time-delayed two-photon absorption-emission technique. As excitation and deexcitation are localized near the inner turning point of the classical orbit (i.e., close to the atomic core) the final state population as a function of the time delay between both laser pulses shows extrema at multiples of the mean classical orbit time. It would be interesting to extend our present analysis to describe the decay of coherence in the wave packet due to coupling to an environment (reservoir).<sup>13,14</sup>

#### ACKNOWLEDGMENT

Support by the Jubiläumsfonds der Österreichischen Nationalbank under project 2604 is gratefully acknowledged.

- <sup>1</sup>L. D. Landau and E. M. Lifshitz, *Quantum Mechanics: Non-relativistic Theory* (Pergamon, New York, 1979).
- <sup>2</sup>J. A. C. Gallas, G. Leuchs, H. Walther, and H. Figger, *Adv. At. Mol. Phys.* **20**, 413 (1985).
- <sup>3</sup>For quantum beat experiments (between fine-structure components of atomic levels) with detection by photoionization see R. Zygan-Maus and H. H. Wolter, *Phys. Lett.* **64A**, 351 (1978); M. P. Strand, J. Hansen, R. L. Chien, and R. S. Berry, *Chem. Phys. Lett.* **59**, 205 (1978); G. Leuchs, S. J. Smith, E. Khawaja, and H. Walther, *Opt. Commun.* **31**, 313 (1979).
- <sup>4</sup>H. Walther, private communication.
- <sup>5</sup>D. Parker and C. R. Stroud, Jr., *Phys. Rev. Lett.* **56**, 716 (1986).
- <sup>6</sup>M. V. Berry and K. E. Mount, *Rep. Prog. Phys.* **35**, 315 (1972).
- <sup>7</sup>W. H. Furry, in *Lectures in Theoretical Physics*, edited by W. E. Brittin, B. W. Downs, and J. Downs (Interscience Publishers, New York, 1963).
- <sup>8</sup>Ph.M. Morse and H. Feshbach, *Methods of Theoretical Physics* (McGraw-Hill, New York, 1953), Vol. I.
- <sup>9</sup>G. Peach, *Mem. R. Astron. Soc.* **71**, 13 (1967).
- <sup>10</sup>M. J. Seaton, *Rep. Prog. Phys.* **46**, 167 (1983).
- <sup>11</sup>S. P. Goreslavskii, N. B. Delone, and V. P. Krainov, *Zh. Eksp. Teor. Fiz.* **82**, 1789 (1982) [*Sov. Phys.—JETP* **55**, 1032 (1982)].
- <sup>12</sup>I. Ya. Bersons, *Zh. Eksp. Teor. Fiz.* **83**, 1276 (1982) [*Sov. Phys.—JETP* **56**, 731 (1982)].
- <sup>13</sup>C. M. Savage and D. F. Walls, *Phys. Rev. A* **32**, 3487 (1985).
- <sup>14</sup>O. Caldeiro and A. J. Leggett, *Phys. Rev. A* **31**, 1059 (1985).